Development and evaluation of a geodetic measurement system for IMU-based high-precision azimuth transfer

Lorenz SCHMID*, Nino KRACHER* and David SALIDO-MONZÚ, Switzerland

*These authors contributed equally to this work

Key words: azimuth transfer, IMU-FOG, autocollimation, geodetic network orientation

SUMMARY

In cases where traversing or a geodetic network do not allow sufficiently accurate azimuth transfer, north-seeking gyroscopes are usually applied. However, these are very sensitive and expensive instruments, and there is a lack of independent control. Based on an idea realized several years ago by TU München and ETH Zürich for network orientation transfer along a vertical shaft in the Gotthard Base tunnel, we have implemented a prototype system for high accuracy azimuth transfer using an Inertial Measurement Unit (IMU) extended with autocollimation. The measurement platform is based on an industrial grade IMU with fiber-optic gyros (FOGs) and an autocollimation prism collocated on a rigid base. Our custom processing software computes the orientation offset between epochs where the platform is at rest, allowing for both 1D and 3D rotation integration and using initial alignment measurements to estimate and compensate for gyroscope drifts and earth rotation. We have additionally developed a numerical simulation tool for assessing the attainable accuracy of such approach depending on the IMU characteristics and for different scenarios. The main area of application, and thus the focus of the investigations, is the transfer of azimuth along a vertical trajectory (e.g. an elevator-shaft) but the applicability of the approach and system to approximately horizontal azimuth transfer (e.g. from above ground to below ground at the portal of a tunnel) is also evaluated and discussed. Measurements performed in an elevator of a multi-story office building yielded a standard deviation of 3.5 mgon of the azimuth difference over a vertical distance of 27 m covered in approximately 30 s, suggesting acceptable performance to provide additional control or to replace north-seeking gyroscopic measurements in some applications. Additional tests to validate the simulation tool and to assess the performance of the system in horizontal azimuth transfer and affected by tilting and vibration are also provided.

Development and evaluation of a geodetic measurement system for IMU-based high-precision azimuth transfer

Lorenz SCHMID*, Nino KRACHER* and David SALIDO-MONZÚ, Switzerland

1. INTRODUCION

North-seeking gyroscopes are the standard solution for azimuth transfer in applications such as complex tunneling where a geodetic network or traversing cannot provide sufficient accuracy (Heunecke & Liebl, 2017). With only a few units worldwide and a single high-end supplier these are, however, expensive and not readily available instruments. This motivates the development of alternatives to provide independent control or even replace the gyroscopic measurements in applications with slightly lower accuracy requirements. ETH Zürich and TU München proposed a solution for azimuth transfer based on inertial measurements. A prototypical platform combining an inertial measurement unit (IMU) with autocollimation (AC) was developed and used during the construction of the Gotthard Base Tunnel, showing promising results by direct comparison with North-seeking gyroscope measurements (Neuhierl et al. 2006). This system is extensively described and analyzed in Neuhierl (2005).

Here, we extend this idea to provide a more general assessment of its potential not only limited to vertical azimuth transfer. We have developed a functional platform based on an industrial-grade IMU with fiber-optical gyros (FOGs) (KVH 1750 IMU), together with a MATLAB-based processing software and structured measurement procedure for inertial azimuth transfer. Additionally, a simulation tool providing realistic IMU data for arbitrary trajectories has been implemented and validated in several measurement tasks by comparison with the actual platform results. This tool provides information on the expected accuracy of the method for different situations and IMU characteristics, enabling quality predictions during the planning phase of measurement tasks where the application of this technique is contemplated.

2. METHODS

2.1 Measurement principle

The main idea of the solution is to determine the change in orientation, in particular of the azimuth, between two resting locations of the measurement platform using an IMU. This is achieved by integrating the angular rates measured by the IMU when the platform is displaced between both stations along an arbitrary trajectory while maintaining an approximately upright position so that most of the rotation occurs about its vertical axis. An example of this measurement principle applied to azimuth transfer between two locations is shown in Figure 1. The orientation change ($\Delta\alpha$) of the platform is derived from the IMU measurements while AC measurements performed using total stations at both resting locations yield the relative orientations of an AC mirror with respect to the geodetic networks close to the respective location. Combining the AC measurements and $\Delta\alpha$ the orientations α_1 and α_2 of the AC mirror at both resting locations can be calculated with respect to the same reference system, thus allowing to transfer the azimuth from the total station at the first location to that one at the second .

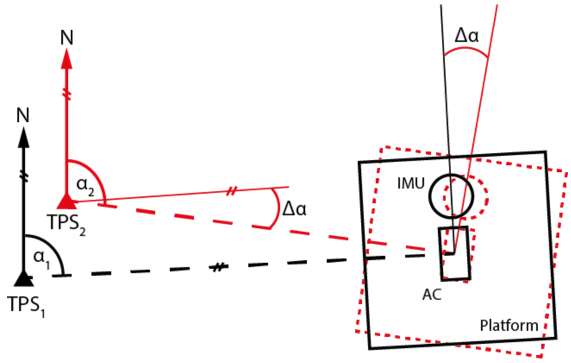

Figure 1: Measurement principle (top view for case of perfectly vertical azimuth transfer between the top (black) and the bottom (red) of a shaft)

2.2 Platform design

The main components of the platform (see Figure 2) are a FOG-IMU, an autocollimation prism, a data logger and a power supply. To observe angular rates a KVH 1750 IMU is used, being approximately one order of magnitude less accurate, hence also less expensive, than the one used in (Neuhierl et al. 2006). The IMU is connected to a notebook for data logging via USB 2.0. The KVH FOG/IMU Interface Software is used for data acquisition.

For transferring the azimuth from the IMU to a total station (TPS) and vice versa an autocollimation prism GAP1 (Wild Herbrugg) is rigidly mounted on the platform. The GAP1, being the heaviest part of the system, is placed at the center of the platform. We have chosen the prism instead of a mirror because it adds convenience in setting up the total station in locations allowing to achieve AC. The prism establishes a reference plane, namely the one perpendicular to the prisms long edge, instead of the reference vector (normal vector) established by an AC mirror. However, the solution is therefore limited to azimuth transfer and requires that the platform be approximately leveled at the resting locations.

Below the platform, a Kern adapter is attached for centering. We used it, in connection with a Kern ground plate for stable setup and leveling of the platform at the resting locations. The plate is mobile, but still heavy enough for a stable set up. Furthermore, it can be easily levelled by the ball head and a built-in bubble level. The power for the IMU and for the data logging is supplied by a rechargeable LiPo battery. To enhance the stability of the platform the components are distributed such that the center of mass coincides approximately with the center of the ground plate.

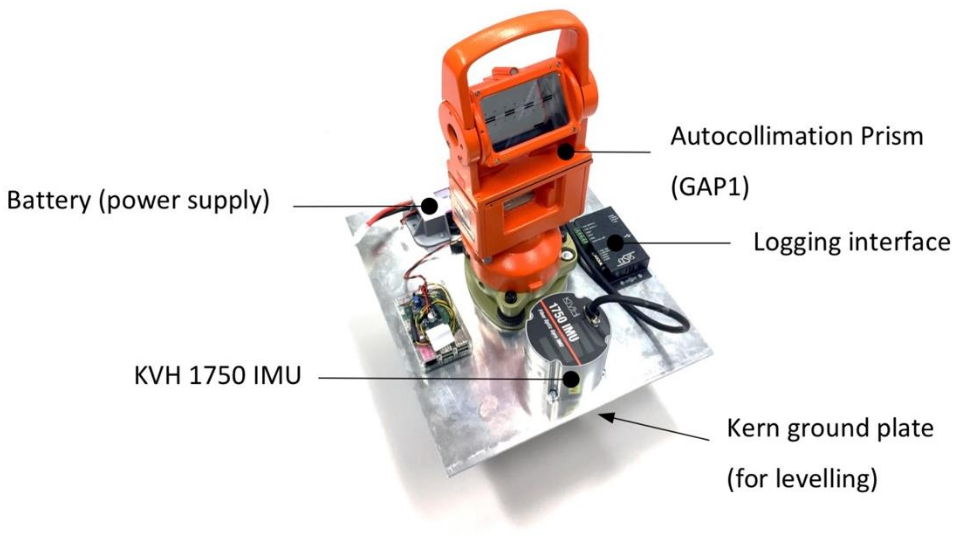

Figure 2: Platform with IMU and autocollimation prism

2.3 Data processing

To process the IMU data and AC measurements, a custom software has been developed in MATLAB. It takes the IMU log files from the KVH FOG/IMU Interface Software in CSV-format and a TXT-file containing the total station measurements as input. The imported IMU measurements are first preprocessed for eliminating outliers based on a user-defined threshold for unlikely angular rates between subsequent epochs and an optional low-pass filter. The static alignment epochs are then detected within the IMU data based on a predefined velocity threshold. An alignment is carried out at the beginning of each IMU measurement set to estimate the angular rate bias offset and optionally compute the north direction using the coupling of earth rotation into the measurements. Finally, rotations and velocities are derived from the measured angular rates and accelerations through integration using the Euler method (Atkinson, 1989), performing both independent (1D) and combined (3D) integration of all the channels.

2.3.1 Motion detection

A motion detection algorithm has been implemented to identify the alignment epochs within the IMU measurements. For the case of a vertical shaft, the accelerometer measurements of the z-axis are integrated once to get the velocity over the period of the movement, which depends on the length of the shaft and velocity of the elevator. For the automatic motion detection, a user-defined velocity threshold is then used to classify the measurements into static and dynamic. Alternatively, the motion detection can be performed manually by selecting the start and end of each alignment epoch in a z-velocity plot.

2.3.2 Alignment

At the beginning of each IMU measurement set, an alignment is carried out to estimate and remove the angular rate bias offset. In the case of a separated 1D integration and assuming that the platform remains vertical during motion, the bias offset of the z-axis rotations, including earth rotation, is simply calculated as the mean value of the static IMU measurements. When the integration is performed combining the 3 axes, earth rotation needs to be subtracted from the measurements before the bias offset is estimated from the rotation rates output by the IMU during the static periods. For the 3D integration, it is additionally important to know the initial orientation of the platform with respect to the north direction and an earth-centered-earth fixed (ECEF) coordinate system such that earth rotation can be properly mapped onto the IMU axes for numeric compensation both during the static periods and during the IMU movement. Assuming that the platform is approximately levelled initially, and its position within the ECEF frame is known, the initial north direction can either be derived from an external azimuth observation onto the GAP1 or estimated less accurately from the observed earth rotation in the angular rates of the x- and y-axes. When an external azimuth is used, the angles between the IMU axes and the GAP1-axes need to be known from a prior calibration. In our case, these angular offsets were acquired beforehand through a TPS-based triangulation of the IMU housing.

2.3.3 Integration

When independent 1D integration is selected, the angular rates of each axis are processed separately based on the Euler method. This simplified approach can be used if the IMU is always approximately leveled during the measurements. If this is not the case a combined 3D integration should be used based on (Jekeli, 2001, p. 112):

$$\begin{pmatrix} \dot{\eta} \\ \dot{\chi} \\ \dot{\alpha} \end{pmatrix} = \begin{pmatrix} 1 & \sin(\eta)\tan(\chi) & \cos(\eta)\tan(\chi) \\ 0 & \cos(\eta) & -\sin(\eta) \\ 0 & \sin(\eta)\sec(\chi) & \sec(\chi) \end{pmatrix} (\boldsymbol{\omega}^{\mathrm{b}} - \mathbf{C}_{\mathrm{n}}^{\mathrm{b}} \boldsymbol{\omega}_{\mathrm{e}}^{\mathrm{n}}) \tag{1}$$

$$\text{with } \mathbf{C}_{\mathrm{b}}^{\mathrm{n}} = \mathbf{R}_3(-\alpha)\mathbf{R}_2(-\chi)\mathbf{R}_3(-\eta) \text{ and } \boldsymbol{\omega}_{\mathrm{e}}^{\mathrm{n}} = [\omega\cos(\Phi), 0, \omega\sin(\Phi)]^T \tag{2}$$

where $\mathbf{C}_{\mathrm{b}}^{\mathrm{n}}$ is the transformation matrix between navigation frame and body frame, defined by the three attitude angles roll (η), pitch (χ) and yaw (α); $\boldsymbol{\omega}^{\mathrm{b}}$ is the axial vector containing the observed angular rates, and $\boldsymbol{\omega}_e^{\mathrm{n}}$ is the axial vector representing the earth rotation ω in the navigation frame for a latitude Φ. Starting from a known orientation, the 3D attitude angles are calculated by integrating their derivatives based on the Euler method. For azimuth transfer, especially the difference in α is of importance.

2.4 Simulation

The simulation consists of two main parts: the generation of simulated measurements and the sequential processing of those. Firstly, a trajectory is defined by positions and attitude angles of the platform with respect to the navigation frame. Accelerations and angular rates are then obtained by differentiation. Next, the IMU noise components are simulated based on the IMU performance specifications and added to the true angular rates. Finally, the simulated data are processed in the same way as the real data (see sec. 2.3). The steps of noise simulation and data processing are then repeated several times for a given trajectory through a Monte Carlo approach in order to facilitate statistical assessment of the results.

2.4.1 Generation of true trajectories

The trajectories are defined by linear interpolation of location and angles between chosen support points. To avoid discontinuities related to the differentiation C^1-continuity of the trajectory is needed. The defined trajectories are smoothed with a moving average filter to guarantee this. For processing, at least two alignment periods have to be included at the beginning and end of the measurements during which the platform is stationary. The output of this stage are a timestamp vector, a vector with discrete positions $(\mathrm{X}, \mathrm{Y}, \mathrm{Z})$ and a vector with attitude angles (η, χ, α).

2.4.2 Differentiation & Earth rotation effect

After computing the attitude rates from the defined attitude angles by numerical differentiation, these are transformed into angular rates using the inverse of (1). During this step, Earth rotation is additionally added to the angular rates based on the current latitude and orientation.

2.4.3 Generation of IMU errors

The three sources of uncertainty of the gyroscopic IMU measurements that are typically dominant for the time scale of the envisioned applications (averaging times up to a few seconds and integration times up to a few minutes) are generated and added to the true angular rates. The first component is bandlimited white noise defined by the angle random walk coefficient ARW $[°/\mathrm{h}/\sqrt{\mathrm{Hz}}]$. The noise power is calculated from its spectral density taking into account the signal bandwidth BW $[\sqrt{Hz}]$, in turn defined by the selected data rate. The noise samples N_{ARW} are generated according to

$$N_{ARW} = \frac{ARW}{3600} \cdot \sqrt{BW} \cdot N(0,1) \qquad [°/\mathrm{s}] \tag{3}$$

where N(0,1) denotes samples of a standard normal distribution.

The second component is a low-frequency noise usually referred to as bias instability [°/h]. When the cutoff time for this contribution is given, it is generated using a first order Gauss Markov signal with appropriate strength and correlation time (Jurado, 2017). Alternatively, when the cutoff time is not defined, the generation of bias instability is approximated by pink noise following a $1/f$ power spectral density.

The last error contribution is the bias offset Δ_0 $[°/h]$, being a constant deviation on the angular rate bias that may change each time the IMU is switched on. For the simulations, the bias offset is assumed to be uniformly distributed, generated for each run and axis as a constant angular bias α_0 calculated from

$$\alpha_0 = \frac{2 \cdot \Delta_0 \cdot U(0,1)}{3600} - \frac{\Delta_0}{3600} \qquad [°/s] \tag{4}$$

Validation results for the two former noise contributions are shown in Figure 3, depicting the Allan deviation calculated for both simulated and empirical data from static measurements along more than 5 h using the IMU mentioned above. According to the IEEE Standard 952 (IEEE, 2008) the angle random walk coefficient is easily obtained by reading the Allan deviation at $\tau = 1$. The bias instability and cutoff time are defined as the point in the Allan deviation where the minimum is reached. However, the accuracy of the Allan deviation decreases towards the end due to fewer samples. An extremely long observation times would be necessary to make an accurate estimate of both the bias instability and the cutoff time, explaining the higher differences in this region. Table 1 shows a comparison between measured and nominal noise parameters, with the IMU used in our tests exhibiting slightly better performance than the typical value provided by the manufacturer.

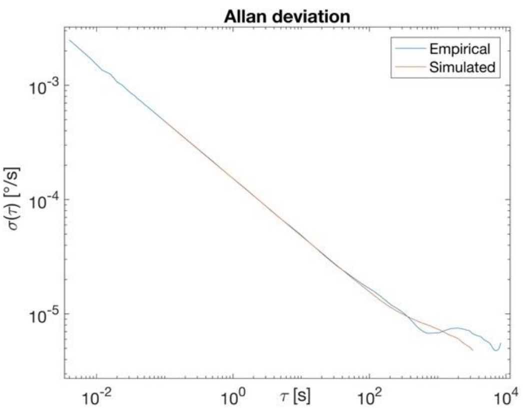

Figure 3: Allan deviation based on observed IMU performance specifications

	Data sheet (KVH, 2016)	Observed
Angle random walk [°/hr/√ Hz]	≤ 0.7	0.55
Bias instability [°/hr], typical	≤ 0.05	≈ 0.025

Table 1: Specified and measured noise performance of IMU

3. RESULTS AND DISCUSSION

Several practical experiments have been carried out to assess the potential of this particular realization of the azimuth transfer platform. They include measurements within an elevator shaft, horizontal transfer with both small and large tilting variations and additional specific measurements to analyze the impact of tilting and earth rotation on the two possible integration methods.

3.1 Vertical shaft

The vertical shaft tests have been performed using an elevator in the HIL building at ETH Zürich. The resulting vertical trajectory is approximately 27 m long. Firstly, the platform is placed in the elevator and levelled. Next, two Leica TS 60 total stations are set up on tripods in front of the elevator doors on the top (H-floor) and on the base (A-floor) of the shaft. For the TPS in H-floor a resection based on prisms with known coordinates is carried out to get horizontal angle measurements with respect to the north direction. In addition, two autocollimation mirrors are setup on the respective floors to periodically check whether the two TPS are stable during the measurements. 10 measurement sets have been carried out in total. Each set consists of an alignment upstairs, a downward ride in the elevator, an alignment downstairs, an upward ride in the elevator and a last alignment upstairs. The elevator ride from H- to A-floor takes approximately 30 seconds. During the alignments of approximately 70 seconds, the IMU is static and therefore the angular rate bias offset can be estimated. Additionally, the azimuth of the GAP1 is observed with the TPS during those static periods.

3.1.1 Spectral analysis

In order to select an appropriate sampling frequency for the IMU measurements in the elevator a spectral analysis of the observed angular rates when the elevator is moving have first been carried out. Measurements with the highest possible sampling rate of 1000 Hz were acquired during an elevator ride and compared with static observations. The power spectral density (PSD) plots of the measurements in the elevator are shown in Figure 4, where it can be seen that no significant dynamics seem to take place above 200 Hz. The biggest part of the dynamics even seems to take place below 50 Hz. Therefore, 250 Hz is chosen as an appropriate sampling rate for further IMU measurements in the elevator.

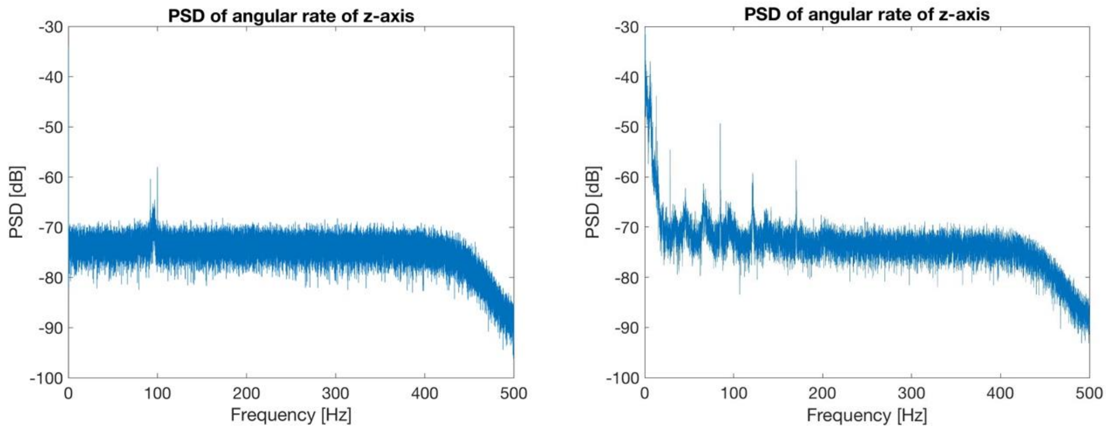

Figure 4: PSD for static measurement (left) and in elevator (right), 1000 Hz sampling frequency

3.1.2 Azimuth transfer

From the 10 measurement sets in the elevator, one had to be removed as it contained a gross error whose reason is unknown. The results from the measurement sets in the elevator are show in Figure 5. The left part of the figure shows the calculated azimuth of the platform while the elevator is travelling down, where very similar dynamics of the elevator can be seen for all measurement sets. The right one shows the residuals of the orientation offsets. The resulting standard deviation (SD) of the orientation offsets between the TPS upstairs and downstairs is 3.5 mgon for both 1D and 3D integration.

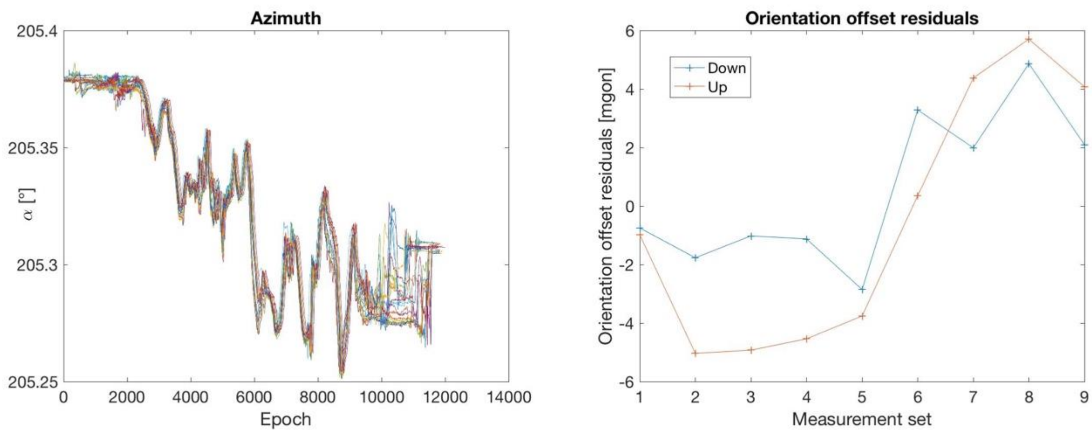

Figure 5: Vertical shaft (empirical, 1D integration)

Using a similar measurement setup as for the empirical experiment, a Monte Carlo simulation with 20 repetitions is carried out. Equivalent results for this simulation are shown in Figure 6. The resulting orientation offset SD is 1.7 mgon for the 1D integration and 1.6 mgon for the combined 3D integration.

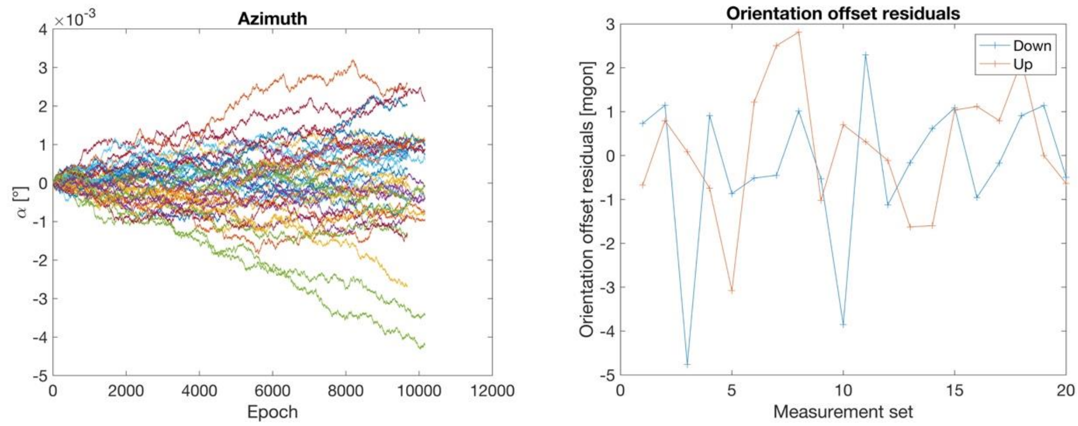

Figure 6: Vertical shaft (simulated, 1D integration)

The empirical SD of the truly measured orientation offsets are slightly higher than those obtained from the simulation. One reason for this could be the vibrations which decrease the accuracy of the empirical IMU measurements and whose effect is not included in the simulations. Furthermore, the measurement uncertainty of the autocollimation measurements is not taken into account in the simulation. However, their contribution is small: from an empirical experiment based on 20 autocollimation measurements with a TS 60 on a GAP1 an autocollimation measurement accuracy of 0.5 mgon is determined.

A closed loop analysis of the empirical data has been additionally carried out. The results for this analysis are shown in Figure 7. The SD of the orientation offsets is 2.3 mgon with both 1D and 3D integration. The mean orientation offset for both cases is about -3.3 mgon, which is statistically not significant but suggests that there are small remaining systematic deviations in the simulation, which may have to be clarified and mitigated in the future.

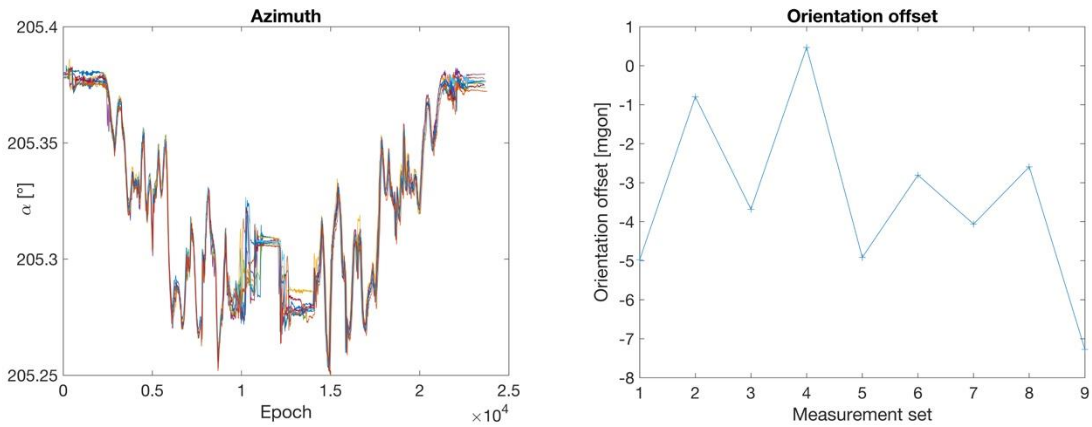

Figure 7: Vertical shaft (closed loop analysis, empirical, 1D integration)

3.2 Horizontal trajectory

The horizontal trajectory measurements are carried out in the 52 m long geodetic metrology laboratory of ETH Zürich. A TPS is set up on a measurement pillar and oriented with respect to the north direction based on two prisms with known coordinates. The analysis is carried out by closed loop measurements. Therefore, only one TPS is needed. The IMU platform is either placed on a trolley or held by hands, to simulate a trolley ride on a rough and uneven underground, while approximately 25 m are walked forth and back in approximately 80 seconds and 60 seconds respectively. At the start and end of the walking, a static alignment of approximately two minutes is carried out with the leveled IMU and the azimuth of the GAP1 is observed by autocollimation.

3.2.1 Trolley

Five measurement sets are carried out with the IMU platform on the trolley, which can be moved precisely along the comparator bench in the lab. The results corresponding to the calculated azimuth and residual orientation offset for the case of 1D integration are shown in Figure 8. For the 1D integration, a mean orientation offset of 4.6 mgon and an orientation offset SD of 25.8 mgon is achieved. For the 3D integration, the mean orientation offset is 12.1 mgon and the SD of the orientation offset is 24.4 mgon. The higher orientation offset in the 3D integration compared to that from the 1D integration is probably due to the integration of noise from the three channels.

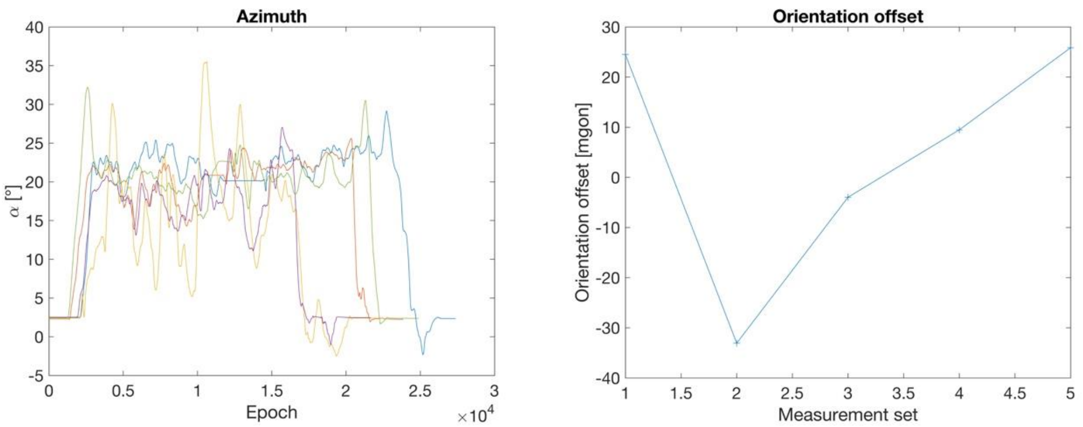

Figure 8: Horizontal shaft (trolley, 1D integration)

3.2.2 Hand held

Six measurement sets are carried out with the hand held IMU platform. Two of them are discarded as they contain gross errors. The equivalent results for this test for 3D integration are shown in Figure 9. The 1D integration the mean orientation offset is -0.96 gon and the SD of the orientation offset 4.8 gon. For the 3D integration, a much smaller mean orientation offset of 21.1 mgon is achieved. The SD of the orientation offset is 78.0 mgon in this case. This clearly shows that 3D integration is of paramount importance in situations where the IMU is not always approximately levelled while moved along the trajectory.

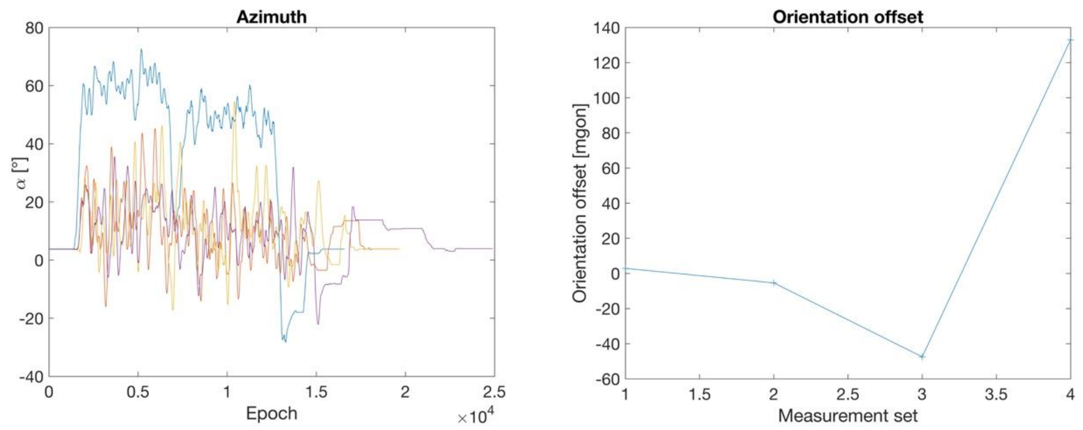

Figure 9: Horizontal shaft (hand held, 3D integration)

3.3 Turning table

For further experiments, the IMU is placed levelled on a turning table, aiming at assessing scale errors. Firstly, an alignment of approximately two minutes is carried out during which the azimuth of the GAP1 is measured. Then, the platform is rotated by 360° in approximately 35 seconds and a second alignment and respective autocollimation measurements are performed. For a second test, the IMU is tilted by -6.5° around the x-axis and -4.2 ° around the y-axis, resulting in a total tilting angle of 7.7°, before being rotated. The purpose of this test is to demonstrate the effect of a tilted platform on the simple 1D integration.

3.3.1 360°- rotation of levelled platform

Based on five measurement sets a mean orientation offset of 9.2 mgon is calculated for the 1D integration. For a 3D integration, the mean orientation offset is slightly higher with 9.5 mgon. The associated orientation offset SD is 7.6 mgon for both 1D and 3D integration. For the mean orientation offset the SD is 3.4 mgon. Based on a 95% confidence interval there seems to be a significant, however small, scale factor. Nevertheless, it is not clear whether this scale factor comes from the IMU measurements or from the numerical integration.

3.3.2 360°- rotation of tilted platform

To demonstrate the effect of a tilted IMU on the sensitivity of the 1D integration two measurement sets are carried out. For the 1D integration this experiment results in a mean orientation offset of -3.6 gon and an orientation offset SD of 0.16 gon. For the 3D integration, the mean orientation offset is heavily reduced to 36.7 mgon and an orientation offset SD of 7.4 mgon. Using the same measurement setup as for the empirical experiment a Monte Carlo Simulation with 20 repetitions is carried out. The resulting mean orientation offset is -3.6 gon for the 1D integration with an orientation offset SD of 1.2 mgon. For the combined 3D integration, the mean orientation offset goes down to -40 mgon with an orientation offset SD of 1.3 mgon.

The expected error of the estimated azimuth change, due to a systematic tilt of the platform can be assessed using the projection of the axial vector of actual rotation onto the tilted z-axis of the platform. The relation is visualized in figure 10.

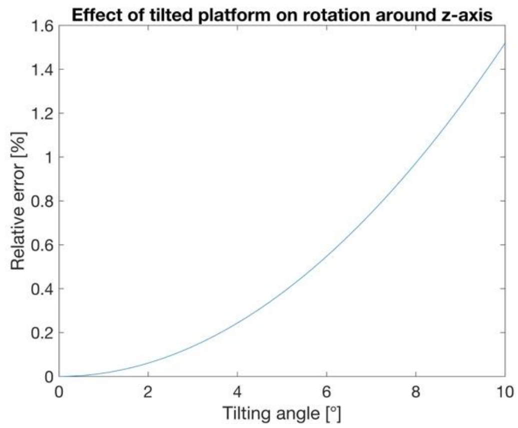

Figure 10: Effect of tilted platform on 1D rotation around z-axis

3.4 Effect of earth rotation

The aim of the last experiment is to demonstrate the influence of earth rotation on the simple 1D integration caused by tilting of the platform after the alignment. Therefore, an alignment of approximately two minutes is carried out with the leveled IMU platform while the azimuth of the GAP1 is measured. The IMU platform is then tilted by -6.5° around the x-axis and -4.2° around the y-axis. After 250 seconds the IMU is tilted back to a level position and the azimuth of the GAP1 is measured again. Based on a single measurement set the resulting orientation offset is 27.8 mgon for the 1D integration and -1.7 mgon for the 3D integration. The results for both cases are depicted in Figure 11.

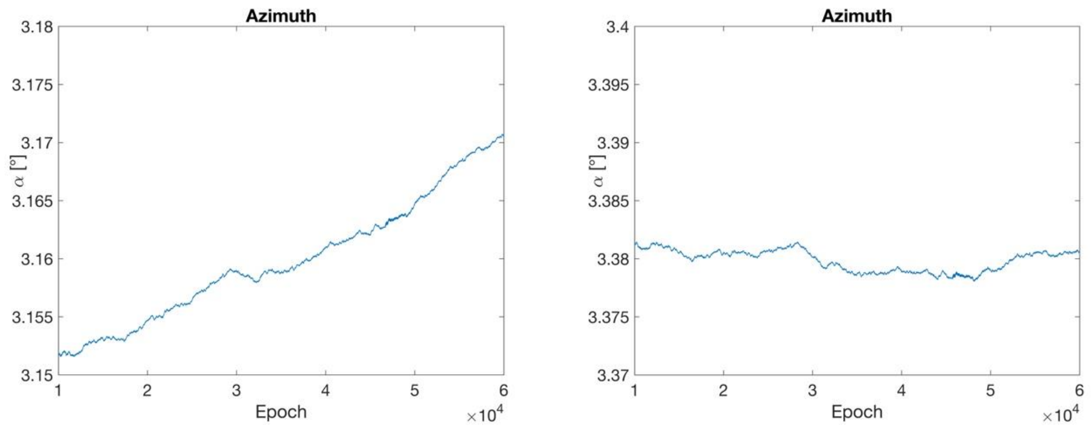

Figure 11: Effect of earth rotation on tilted platform using 1D integration (left) and 3D integration (right)

Based on the same measurement setup a Monte Carlo Simulation with 20 repetitions is carried out. The resulting mean orientation offset is 26.7 mgon for the 1D integration and -2.3 mgon for the 3D integration. The respective orientation offset SD is 5.8 mgon for the 1D integration and 5.1 mgon for the 3D integration. These results again highlight the advantage of the 3D integration for situations when the platform cannot be kept approximately leveled along the trajectory.

4. CONCLUSION

A prototype for inertial-based azimuth transfer has been developed using an industrial-grade IMU and autocollimation. The system includes a user-friendly data processing tool implemented in MATLAB that allows for signal pre-processing, automatic initial alignment for bias compensation and integration of the IMU data both in 1D, i.e. with respect to an individual axis, and 3D, i.e. taking rotations about all axes into account. A simulation tool has been additionally implemented to generate realistic IMU data from an assumed trajectory, which enables assessing the performance of different IMU types for different measurement tasks. The system has been evaluated in different situations and compared to the simulation results for validation. For the KVH 1750 IMU and azimuth transfer between locations occupied within about 30 to 60 seconds, the empirical measurements and simulated values show good agreement. The residual differences on the order of about 1 mgon can be explained by effects like vibrations and autocollimation uncertainties not included in the simulation.

The investigation showed that the designed IMU platform is able to transfer the azimuth with accuracies on the order of a few mgons between two locations where the platform is at rest and nearly levelled. This level of accuracy has been achieved for situations where the transport of the platform between the two locations lasted up to about 80 seconds. These results indicate that the method originally published in Neuhierl (2005) may be applicable for independent control of a north-seeking gyroscope when realized with a less costly and less accurate fiber-optic gyro-based IMU. In applications with slightly lower accuracy requirements, the platform may even replace the gyro. However, the results also clearly showed the limitations due to 1D processing of single-axis rotations only. The field of potential applications is significantly extended by using 3D integration, as the platform does not need to be kept approximately levelled during transport in this case. The algorithm implemented herein could yield accuracies at the mgon level with platform tilts up to about 10° during transport.

Future work should focus on fully exploiting this 3D capability and relaxing the constraints regarding the trajectory between the locations where the platform is at rest. This might facilitate use of such a platform for nearly horizontal azimuth transfer from above ground to below ground through tunnel portals or highly economic azimuth transfer through complex underground spaces. Kalman filtering could allow improving the results through better noise mitigation and more accurate modelling of non-white noise behavior of the IMU.

REFERENCES

Atkinson, K. A. (1989). *An Introduction to Numerical Analysis.* New York: John Wiley & Sons.

Heunecke, O., & Liebl, W. (2017). Accuracy and reliability of gyro measurements at today's tunnelling projects. *Journal of Applied Geodesy 12*.

IEEE. (2008). *IEEE Standard Specification Format Guide and Test Procedure for Single-Axis Interferometric Fiber Optic Gyros.*

Jekeli, C. (2001). *Inertial Navigation Systems with Geodetic Applications.* Berlin: de Gruyter.

Jurado, J. (2017). *mathworks.com.* Retrieved 11 27, 2017, from https://ch.mathworks.com/matlabcentral/fileexchange/61777-tools-for-inertial-allan-variance-analysis-and-simulation

KVH. (2016). *kvh.com.* Retrieved 11 30, 2017, from http://www.kvh.com/Military-and-Government/Gyros-and-Inertial-Systems-and-Compasses/Gyros-and-IMUs-and-INS/IMUs/1750-IMU.aspx

Neuhierl, T. (2005). *Eine neue Methode zur Richtungsübertragung durch Koppelung von Inertialmesstechnik und Autokollimation.* Institut für Geodäsie, GIS und Landmanagement. Technischen Universität München.

Neuhierl, T., Schnädelbach, K., Wunderlich, T., Ingensand, H., & Ryf, A. (2006). *How to Transfer Geodetic Network Orientation Through Deep Vertical Shafts – An Inertial Approach.* Munich, Germany: XXIII FIG Congress.

BIOGRAPHICAL NOTES

Lorenz Schmid and **Nino Kracher** are MSc students of Geomatic Engineering at ETH Zürich. They received their BSc in Geomatic Engineering and Planning by ETH Zürich in 2015. Their areas of specialization are Geomatic Engineering & Photogrammetry and Space Geodesy & Navigation. **David Salido-Monzú** received his PhD by the University of Alcalá (Spain) and is currently postdoctoral researcher at the Institute of Geodesy and Photogrammetry of ETH Zürich. His main areas of research are optical metrology and electronic instrumentation for measurement applications.

CONTACTS

Lorenz Schmid, Nino Kracher, David Salido-Monzú
ETH Zürich
Institute of Geodesy and Photogrammetry
SWITZERLAND
Email: schmidl@student.ethz.ch, krachern@student.ethz.ch, david.salido@geod.baug.ethz.ch